International Journal of Applied Sciences, Research, and Innovation

OPEN ACCESS

FULL PAPER | IJASRI | OPEN

Adaptive Thermal Operator Learning for Near-Wellbore Recovery and Early Drill Stem Test Flow Inference after Drilling Circulation

Mohamed Ould Salem[1], **Ahmed Cheikh Sidya**[2], **Sidi Mohamed Lemine**[3]

[1]Université des Sciences, de Technologie et de Médecine de Nouakchott, Avenue Gamal Abdel Nasser, Nouakchott 5026, Mauritania
[2]Institut Supérieur des Études Technologiques de Rosso, Route de Boghé, Rosso 16005, Mauritania
[3]École Normale Supérieure de Nouakchott, Rue de l' Indépendance, Tevragh-Zeina, Nouakchott 5012, Mauritania

Abstract

Background temperature disequilibrium created during drilling circulation can remain around the wellbore for a substantial period after pumping stops. In petroleum, gas, and geothermal wells, this persistence complicates the interpretation of post-circulation flow behavior because the fluid entering the wellbore during early cleanup or testing may sample a thermally disturbed region rather than the undisturbed formation. The difficulty becomes more pronounced when a well experiences multiple operational transitions, including circulation, shut-in recovery, perforation, early inflow, and multirate test periods, before thermal stabilization is achieved. This paper develops a distinct operator-learning framework for estimating near-wellbore thermal recovery and using that estimate for early drill stem test flow inference. The proposed model combines radial heat diffusion, axial wellbore energy transport, multientry inflow mixing, and sequential state updating in a regime-aware reduced-order structure. A physics-constrained memory mechanism is introduced so that information learned during circulation and shut-in is preserved when the well transitions into flow, thereby reducing the loss of thermal history that commonly biases early-time interpretation. The framework treats the disturbed temperature field as a latent state, infers its evolution from pressure, temperature, and rate data, and links that state directly to entering fluid temperature and transient flow estimation. The paper derives the governing equations, constructs the reduced dynamical representation, develops an online estimation strategy, analyzes stability and identifiability, and proposes a field-oriented validation protocol. The resulting formulation is intended to improve early-time test interpretation in wells where near-wellbore thermal recovery remains incomplete and where fixed-regime inference is vulnerable to systematic error.

1. Introduction

Thermal transients near the wellbore are often treated as secondary effects during post-drilling interpretation, yet in many wells they are integral to the physical state sampled during the earliest stages of testing and cleanup [30]. Circulation modifies the energy balance of the wellbore and the surrounding rock by exposing the formation to a moving fluid whose temperature differs from the native geothermal condition. The immediate result is a disturbed radial temperature field centered on the well. The longer-term result is a recovery process whose timescale is set by conduction, near-wellbore storage, and subsequent flow operations. If perforation and testing occur before this recovery is complete, then the first inflowing fluids do not arrive at a temperature representative of the undisturbed formation. Instead they carry a thermal signature inherited from the disturbed near-wellbore zone. That signature influences fluid properties, apparent inflow behavior, and the interpretation of rate, phase state, and deliverability. The problem is not only one of thermal description. It is an inverse problem in which the current measurements depend on an unobserved thermal history generated by earlier operational stages.

The practical difficulty is sharpened by the fact that the well rarely remains in a single mode while the thermal field recovers. A typical sequence involves active circulation, cessation of flow and shut-in, possibly a waiting interval, perforation, cleanup, drawdown, a buildup, and sometimes additional rate changes or further circulation-related interruptions. The governing equations are physically connected across these operations, but the dominant terms differ from regime to regime [23]. During circulation, the formation experiences imposed thermal forcing from the wellbore and the axial transport of energy in the fluid column is central. During shut-in, the thermal field tends to evolve diffusively, and the near-wellbore zone relaxes toward the far-field state. During production or test flow, the entering fluid temperature depends on a moving radial weighting over the disturbed rock, while the wellbore energy equation is influenced by multientry mixing, compressibility, and transient mass balance. A model that assumes a single stationary regime for all these periods is structurally misaligned with the operation it seeks to interpret.

In field practice, analysts often compensate by switching manually between specialized submodels or by calibrating one model after another over selected windows. That strategy can work when data are abundant, the well is simple, and

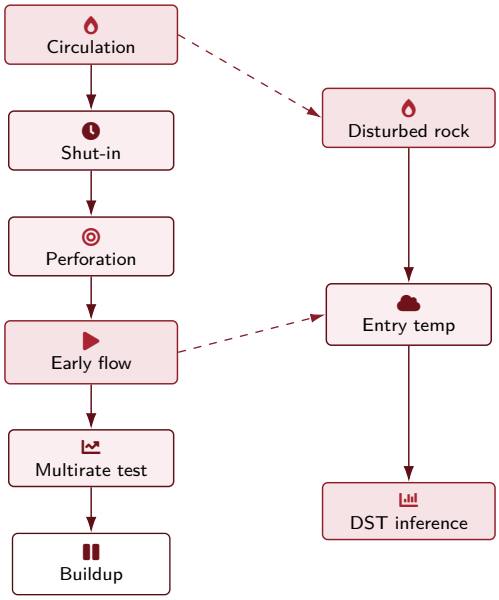


Figure 1. Operational sequence for circulation-disturbed wells. The left chain tracks field actions, while the right chain shows the latent thermal carryover that survives regime transitions and conditions early entry-temperature and drill stem test interpretation.

Table 1. Key thermal variables used in the near-wellbore recovery model

Symbol	Unit	Description
$T_f(r, z, t)$	K	Formation temperature field in radial–axial coordinates
$T_w(z, t)$	K	Wellbore fluid temperature along the completion interval
$T_\infty(z)$	K	Undisturbed geothermal temperature profile
$\theta(r, z, t)$	K	Thermal disturbance relative to equilibrium
r_w	m	Effective wellbore radius
r_b	m	Outer radius of computational domain

the operating history is mild. It becomes fragile when the same set of uncertain parameters influences several stages simultaneously, when the near-wellbore thermal field remains latent, and when the observational meaning of temperature changes between one regime and the next. A temperature decline during circulation, for example, need not mean the same thing as a temperature decline during early flow. In the former case it may primarily reflect axial wellbore transport and boundary forcing. In the latter case it may reflect the radial thermal structure of the formation and the relative contribution of multiple entry points. A robust framework should therefore retain what is learned in one regime, but reinterpret that knowledge appropriately when the regime changes [14].

This requirement can be stated more precisely as a sequential learning problem with memory. The model must estimate a hidden thermal state, infer uncertain physical parameters, and update its dynamics when operational mode changes occur, all without discarding knowledge extracted earlier from the same well. Hasan et al. (2024) demonstrated in the near-wellbore cooling and drill stem test setting that circulation-induced thermal disturbance can persist after shut-in and materially affect early inflow temperature and flow-rate interpretation [17]. The present paper adopts that field context but develops a different methodological emphasis: it formulates the problem as adaptive operator learning for a regime-changing thermal-flow system and focuses on how historical thermal information can be preserved and reused during online test interpretation.

The central proposition is that the disturbed near-wellbore temperature field should be treated as a latent dynamical object rather than as a one-time correction. Once represented this way, a natural architecture emerges. A shared thermal operator describes the diffusion-dominated backbone of radial recovery. Regime-conditioned perturbations account for circulation forcing, early inflow advection, multirate test effects, and changes in measurement structure. A reduced basis permits the radial field to be estimated from sparse downhole data. A memory mechanism stores physically meaningful summaries of previous thermal states, operator corrections, and representative trajectories, so that the system can re-

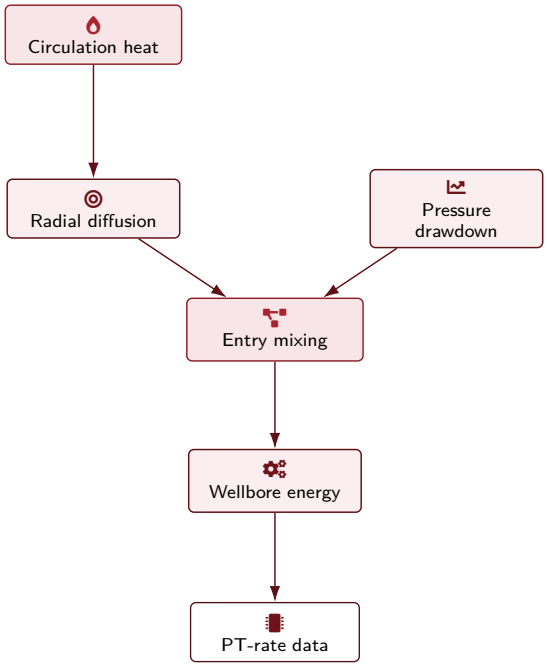


Figure 2. Coupled physics block view. Circulation-induced thermal forcing creates a disturbed radial field; pressure drawdown selects the sampled region; entry mixing transfers that history into the wellbore energy balance and finally into pressure-temperature-rate observations.

Table 2. Primary thermal transport parameters

Parameter	Symbol	Physical meaning
Effective conductivity	k_e	Composite rock–fluid heat conduction coefficient
Volumetric heat capacity	$(\rho c)_e$	Effective storage capacity of porous medium
Thermal diffusivity	α	Ratio $k_e/(\rho c)_e$ governing radial recovery speed
Heat transfer coefficient	h_c	Wellbore–formation convective exchange parameter
Overall transfer coefficient	U	Combined conductive and convective wellbore heat transfer

visit or reuse them as later operational segments unfold. The result is a model that is neither purely deterministic simulation nor purely generic machine learning. It is a hybrid inverse framework in which the governing physics define the state representation and admissible transitions, while online adaptation determines how strongly each regime-specific correction should be activated [5].

The paper has several objectives. The first is to derive a mathematically coherent model for radial near-wellbore thermal recovery and its effect on early inflow temperature during drill stem testing. The second is to couple that model to an operator-based reduced-order state space capable of supporting online inference. The third is to introduce a physics-constrained memory principle that protects previously learned thermal structure from being overwritten when the operational regime changes. The fourth is to analyze stability, identifiability, and error propagation in the resulting learned thermal dynamics. The fifth is to show how such a model can be implemented numerically in a way that remains compatible with field data streams, multirate schedules, and incomplete observation. In keeping with the operational focus of the problem, the paper does not seek to maximize abstract predictive performance alone. It seeks to improve early-time interpretation under the specific conditions created by prior circulation and incomplete thermal recovery.

The remainder of the manuscript is organized as follows. The next section formulates the physical problem and derives the coupled formation-wellbore heat and flow equations in a form suitable for reduction. The following section develops a thermal entry-temperature inversion model that links the latent radial field to wellbore inflow diagnostics [6]. A subsequent section introduces the regime-aware latent operator representation. The paper then develops a continual learning and memory-consolidation framework designed for sequential well operations, followed by a section on state estimation, multientry flow inference, and rate reconstruction. Stability, identifi-

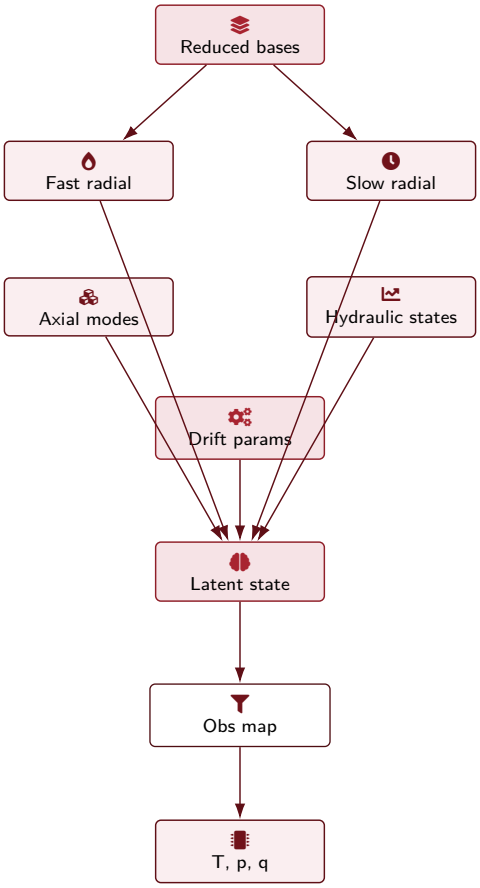


Figure 3. Reduced latent-state construction. Fast and slow radial modes preserve the disturbed near-wellbore thermal field, axial and hydraulic summaries complement the state, and a regime-dependent observation map converts the reduced state into measurable temperature, pressure, and rate signals.

ability, and convergence issues are addressed afterward. The later sections describe numerical realization and field-oriented experimental design, and the paper concludes with a discussion of implications for thermal interpretation and drill stem test diagnostics.

2. Governing Thermal and Flow Equations for the Disturbed Near-Wellbore Zone

The physical system considered here consists of a wellbore intersecting a porous formation whose undisturbed temperature $T_\infty(z)$ may vary with depth. During circulation, the wellbore fluid exchanges heat with the formation, thereby creating a disturbed region around the wellbore in which the temperature differs from T_∞. The analysis focuses on the tested interval, where the disturbed field materially influences the temperature of fluids entering the wellbore during subsequent operations. To retain the essential physics while keeping the inference problem tractable, the model adopts an axisymmetric radial description in the formation coupled to a reduced axial energy balance in the wellbore.

Let r denote radial distance from the well axis and z the axial coordinate over the tested interval. The formation temperature is $T_f(r, z, t)$, the wellbore fluid temperature is $T_w(z, t)$, the formation pressure is $p_f(r, z, t)$, and the wellbore pressure is $p_w(z, t)$. The near-wellbore thermal disturbance is represented by [29]

$$\theta(r, z, t) = T_f(r, z, t) - T_\infty(z). \tag{1}$$

The relevant radial interval begins at the effective wellbore radius r_w and extends outward until the disturbance decays to negligible magnitude relative to measurement resolution or interpretation sensitivity. The exact outer boundary is not physically sharp, but for reduced-order modeling it is useful to define an effective radius $r_e(t)$ or a fixed computational boundary r_b large enough that $\theta(r_b, z, t) \approx 0$.

When formation inflow is negligible, the thermal evolution is governed primarily by radial diffusion. Allowing for effective rock-fluid heat storage, the energy equation can be written as

$$(\rho c)_e \frac{\partial T_f}{\partial t} = \frac{1}{r}\frac{\partial}{\partial r}\left(k_e r \frac{\partial T_f}{\partial r}\right) + q_{wf}(r, z, t), \tag{2}$$

where $(\rho c)_e$ is the effective volumetric heat capacity of the porous medium, k_e is effective thermal conductivity, and q_{wf} is the volumetric source term induced by heat exchange with the wellbore or by reduced-order forcing used to represent circulation effects. Expressed in terms of the disturbance θ, and assuming T_∞ is stationary over the time window of

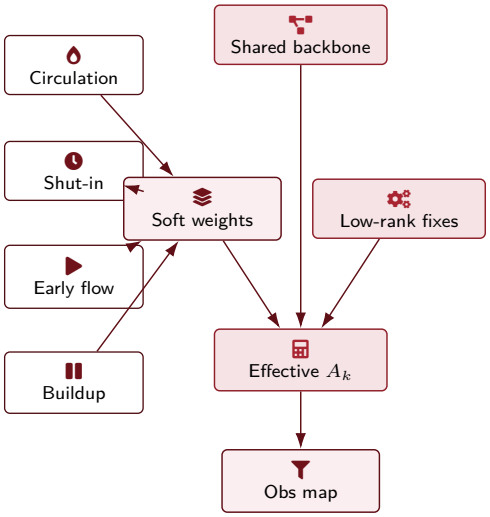


Figure 4. Regime-aware operator decomposition. A shared diffusion-centered backbone is retained across operations, while soft regime weights activate low-rank operator corrections that adapt the transition and observation structure without rebuilding the full model at each operational change.

Table 3. Operational regimes considered in the adaptive framework

Regime	Dominant physics	Typical observations
Circulation	Axial advection and forced heat exchange	Strong wellbore temperature gradients
Shut-in recovery	Radial conduction in formation	Gradual thermal relaxation
Early flow	Inflow-weighted thermal sampling	Rapid temperature response at entry
Multirate testing	Coupled hydraulic–thermal dynamics	Rate-dependent temperature shifts
Buildup period	Pressure recovery with residual cooling	Slow temperature stabilization

interest, the recovery equation becomes

$$\frac{\partial \theta}{\partial t} = \alpha \left(\frac{\partial^2 \theta}{\partial r^2} + \frac{1}{r} \frac{\partial \theta}{\partial r} \right) + s_\theta(r, z, t), \tag{3}$$

where $\alpha = k_e/(\rho c)_e$ is thermal diffusivity and s_θ is the reduced source associated with boundary forcing.

During circulation, the thermal boundary condition at the wellbore is driven by the temperature of the moving wellbore fluid. A mixed boundary condition is appropriate:

$$-k_e \left. \frac{\partial T_f}{\partial r} \right|_{r=r_w} = h_c(z,t) \left(T_f(r_w, z, t) - T_w(z,t) \right), \tag{4}$$

where h_c is an effective wellbore-to-formation heat-transfer coefficient. The wellbore temperature itself evolves under axial advection, internal energy storage, and exchange with the formation. If a single effective flowing stream is considered over a completion segment, the corresponding energy balance is

$$\frac{\partial}{\partial t} \left(\rho_w A_w c_{p,w} T_w \right) + \frac{\partial}{\partial z} \left(\dot{m} h_w \right) = UP \left(T_f(r_w^+, z, t) - T_w \right) + Q_s, \tag{5}$$

where A_w is flow area, $\dot{m}$ mass flow rate, h_w enthalpy, U overall transfer coefficient, P wetted perimeter, and Q_s collects mechanical, mixing, and source terms. For offshore or long completion intervals a two-stream annulus-tubing system may be needed, but for the present inferential development the reduced single-stream form is sufficient [18].

Once circulation stops, the well enters a shut-in or reduced-flow thermal recovery phase. In that regime the axial advective term weakens, and the formation disturbance relaxes toward equilibrium. The initial condition for shut-in is the circulation-generated thermal field $\theta(r, z, t_s)$, where t_s is the shut-in start time. A major challenge is that $\theta(r, z, t_s)$ is not directly observed. It must either be inferred from the prior circulation history or represented through a surrogate parameterization. A common analytical simplification approximates the net circulation effect as a line-source or ring-source disturbance. If the cumulative heat extracted from the formation over the tested interval is $Q_c(z)$, then a stylized post-

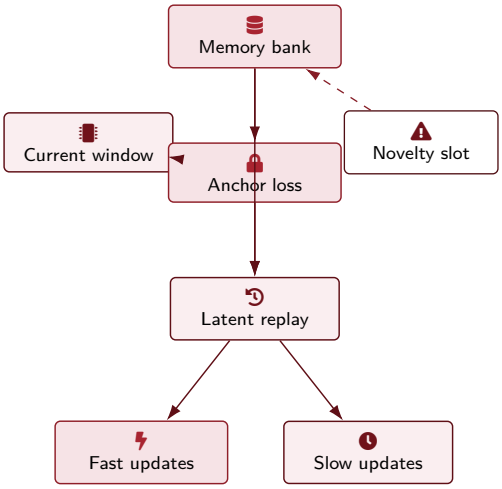


Figure 5. Physics-constrained continual learning. Historical operator structure is protected through anchoring and latent replay, a novelty slot screens unfamiliar behavior before consolidation, and update speed is split so regime-sensitive corrections remain agile while the thermal backbone changes slowly.

Table 4. Reduced-order latent state components

State component	Symbol	Interpretation
Fast radial thermal modes	a_f	Near-wall cooling or heating structure
Slow radial thermal modes	a_s	Broader formation recovery dynamics
Wellbore temperature modes	b	Axial thermal imbalance inside the well
Hydraulic allocation states	q	Entry-point flow partition and pressure summaries
Parameter drift variables	ϑ	Slowly varying uncertain physical parameters

circulation thermal field can be written as a diffusion kernel convolved with that forcing:

$$\theta(r,z,t) = -\int_0^{t_s} \frac{q_c(z,\tau)}{4\pi k_e} E_1\left(\frac{r^2}{4\alpha(t-\tau)}\right) d\tau, \quad t > t_s, \tag{6}$$

where E_1 is the exponential integral. This representation is not exact for all circulation geometries, but it provides an interpretable reduced-order map from circulation history to thermal disturbance. It also shows immediately why the near-wellbore zone can remain disturbed long after pressure effects have partially relaxed: the recovery kernel decays diffusively and therefore slowly in the radial coordinate.

When the formation begins to flow, the problem changes qualitatively [26]. The entering fluid temperature depends on the radial thermal field sampled by streamlines feeding the well. For a single-phase radial inflow, the mass balance and Darcy law may be written as

$$\frac{\partial}{\partial t}(\phi\rho) + \frac{1}{r}\frac{\partial}{\partial r}(r\rho v_r) = 0$$
$$v_r = -\frac{k_r}{\mu}\frac{\partial p_f}{\partial r}, \tag{7}$$

where k_r is radial permeability, μ is viscosity, and ρ may depend on both p_f and T_f. The energy equation for the flowing porous medium then becomes

$$(\rho c)_e \frac{\partial T_f}{\partial t} + (\rho c)_\ell v_r \frac{\partial T_f}{\partial r} = \frac{1}{r}\frac{\partial}{\partial r}\left(k_e r \frac{\partial T_f}{\partial r}\right) + q_{wf}(r,z,t). \tag{8}$$

Very near the wellbore, the advective term influences which part of the disturbed radial field contributes most strongly to the entering fluid temperature. Early-time inflow is disproportionately sensitive to the thermal structure close to r_w, while later inflow progressively samples larger radii as the pressure transient expands.

To connect the radial field to the temperature of fluid entering the well, it is convenient to define an inflow-weighted temperature functional. Let $w(r,t)$ be a positive kernel representing the fraction of entering mass at time t that has recently sampled radius r. Then

$$T_{in}(z,t) = \frac{\int_{r_w}^{r_b} w(r,z,t) T_f(r,z,t)\, dr}{\int_{r_w}^{r_b} w(r,z,t)\, dr}. \tag{9}$$

The kernel depends on the pressure and mobility fields and,

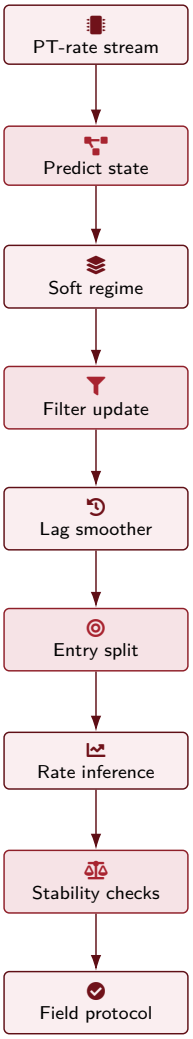


Figure 6. Sequential interpretation workflow. Streaming measurements drive prediction, regime weighting, filtering, smoothing, multientry allocation, and early-time rate inference, after which stability checks and field-oriented validation determine whether the inferred thermal-flow state remains physically credible.

in multientry situations, on the relative contribution of each perforated interval. This expression highlights why early temperature interpretation is history dependent. The entering temperature is not a local state variable; it is an observable generated by applying a time-varying functional to the latent disturbed field [7].

The wellbore energy equation must then incorporate inflow enthalpy. For multiple entry points z_j, the reduced axial form becomes

$$\frac{\partial}{\partial z}\left(\dot{m}(z,t)h_w(z,t)\right) = U(z,t)P(z)\left(T_f(r_w^+,z,t) - T_w(z,t)\right) + \sum_{j=1}^{N_p} \dot{m}_j(t)h_{in,j}(t)\delta(z-z_j) + Q_\ell(z,t), \tag{10}$$

where $h_{in,j}(t)$ is determined by $T_{in}(z_j,t)$, N_p is the number of active entry points, and Q_ℓ accounts for additional longitudinal effects. When rate changes are imposed during a multirate DST, $\dot{m}_j(t)$ changes while the thermal field may still be recovering from previous operations. The energy and pressure dynamics are therefore path dependent even if the imposed flow schedule is known exactly.

These coupled equations form the physical basis of the inverse problem addressed later. They also suggest the proper state variables for reduction: radial thermal modes in the formation, selected wellbore temperature modes, pressure-related state summaries, and uncertain parameters such as effective diffusivity, heat-transfer coefficients, and mobility multipliers. The next section constructs a reduced model specifically designed to invert the entering temperature and flow response from incomplete measurements.

3. Thermal Entry-Temperature Inversion and Reduced Radial State Representation

The direct PDE system described above is too high dimensional and too weakly observed to support efficient online

Table 5. Operator components in the regime-aware dynamical system

Operator term	Symbol	Functional role
Backbone transition operator	$\bar{A}_k$	Shared thermal–flow dynamics across regimes
Control forcing matrix	$\bar{B}_k$	Mapping from operational inputs to state evolution
Observation operator	$\bar{H}_k$	Baseline mapping from latent state to measurements
Regime correction operator	$R_k(s_k)$	Low-rank adjustments for operational changes
Observation correction term	$M_k(s_k)$	Regime-dependent measurement interpretation

Table 6. Memory bank structure for continual learning

Memory element	Symbol	Stored information
State centroid	$\bar{x}_m$	Representative latent thermal-flow state
Covariance summary	Σ_m	Variability of stored trajectories
Operator snapshot	$\bar{A}_m$	Representative transition operator
Observation mapping	$\bar{H}_m$	Measurement relationship for the regime
Trajectory fragments	$\mathcal{T}_m$	Compressed historical dynamics for replay
Importance matrix	Ω_m	Sensitivity of prediction to parameter changes

adaptation without reduction. What is needed is a finite-dimensional representation of the disturbed near-wellbore zone that preserves the aspects of the radial thermal field most relevant to early inflow and wellbore temperature interpretation. The reduction developed here is not a generic compression. It is chosen to preserve the mapping from circulation-induced disturbance to entering fluid temperature and from entering temperature to measurable wellbore response.

Let the thermal disturbance in a tested interval be expanded in a radial basis:

$$\theta(r,t) = \sum_{i=1}^{m} a_i(t)\,\varphi_i(r), \tag{11}$$

where the basis functions $\varphi_i(r)$ may be selected as eigenfunctions of the radial diffusion operator, finite-volume hat functions over logarithmic radial partitions, or orthonormalized snapshots from circulation and recovery simulations [21]. The coefficients $a_i(t)$ become part of the latent state. A diffusion-adapted basis is particularly attractive because, in the absence of inflow, the modal dynamics are approximately diagonal or weakly coupled. If the φ_i satisfy

$$\alpha\left(\varphi_i''(r) + \frac{1}{r}\varphi_i'(r)\right) = -\lambda_i \varphi_i(r), \tag{12}$$

under suitable boundary conditions, then the modal coefficients evolve approximately as exponentially damped processes during shut-in. This yields a natural reduced-order description of recovery:

$$\dot{a}_i(t) = -\lambda_i a_i(t) + b_i(t), \tag{13}$$

where $b_i(t)$ represents forcing induced by the wellbore boundary condition or by inflow-related advection.

The entering fluid temperature can also be expressed in this basis. Using the inflow-weighted functional introduced earlier,

$$T_{in}(t) = T_\infty + \frac{\sum_{i=1}^{m} a_i(t) \int_{r_w}^{r_b} w(r,t)\varphi_i(r)\,dr}{\int_{r_w}^{r_b} w(r,t)\,dr}. \tag{14}$$

Defining the time-varying projection vector

$$c_i(t) = \frac{\int_{r_w}^{r_b} w(r,t)\varphi_i(r)\,dr}{\int_{r_w}^{r_b} w(r,t)\,dr}, \tag{15}$$

one obtains a compact relation

$$T_{in}(t) = T_\infty + c(t)^\top a(t). \tag{16}$$

This equation is central to the inverse formulation [13]. It shows that the unobserved radial field influences the entering fluid temperature through a low-dimensional linear functional whose coefficients vary with the flow regime. During early flow the vector $c(t)$ emphasizes near-wall modes. At later times it shifts weight outward. Under rate changes, $c(t)$ may change abruptly while the coefficients $a(t)$ remain continuous. The learner therefore needs to adapt the observation operator

Table 7. Sequential estimation quantities

Estimator variable	Symbol	Description
Predicted state	$\hat{x}_{k\|k-1}$	Model-based forecast before measurement update
Filtered state	$\hat{x}_k$	Posterior latent estimate after correction
Prediction covariance	$P_{k\|k-1}$	Uncertainty of predicted state
Kalman gain	K_k	Measurement weighting in state update
Innovation vector	ν_k	Residual between observed and predicted data

Table 8. Multientry inflow variables in the wellbore energy balance

Quantity	Symbol	Interpretation
Entry-point inflow rate	$\dot{m}^{(j)}$	Mass flow contribution from perforation j
Total well rate	$\dot{m}_{tot}$	Aggregate production during test period
Inflow temperature	$T_{in}^{(j)}$	Formation fluid temperature entering the well
Allocation variable	$\zeta^{(j)}$	Log-weight controlling flow distribution
Entry enthalpy	$h_{in}^{(j)}$	Thermal energy carried by inflowing fluid

more quickly than the underlying thermal state.

To include wellbore transport, define an axial reduced basis for the fluid temperature over the tested interval:

$$T_w(z,t) = \bar{T}_w(z) + \sum_{j=1}^{n} b_j(t)\,\psi_j(z), \tag{17}$$

where $\psi_j(z)$ are axial basis functions and $b_j(t)$ are wellbore thermal coefficients. The combined latent state is then

$$x(t) = \begin{bmatrix} a(t) \\ b(t) \\ q(t) \\ \vartheta(t) \end{bmatrix}, \tag{18}$$

where $q(t)$ denotes selected hydraulic states or inflow summaries and $\vartheta(t)$ denotes slowly varying uncertain parameters. In practice $q(t)$ may contain bottom-hole pressure correction terms, multientry allocation variables, or reduced pressure-diffusion coefficients. The inclusion of $\vartheta(t)$ in the state rather than in a separate static parameter vector is deliberate: several quantities that would be constant in an idealized model appear time varying in real data because of operational changes, uncertain completion effects, or unresolved multiphase behavior [2].

Galerkin projection of the formation and wellbore equations onto the chosen bases yields a reduced dynamical system. In abstract form,

$$\dot{x}(t) = A_{s(t)}x(t) + B_{s(t)}u(t) + f_{nl}(x(t),u(t),s(t)) + \xi(t), \tag{19}$$

where $s(t)$ is the operating regime, $A_{s(t)}$ is a regime-dependent linear operator, $B_{s(t)}$ is the forcing operator, f_{nl} contains nonlinear couplings due to property variation or multientry mixing, and $\xi(t)$ represents model error. The observation model takes the form

$$y(t) = C_{s(t)}x(t) + D_{s(t)}u(t) + g_{nl}(x(t),u(t),s(t)) + \eta(t). \tag{20}$$

This representation makes clear that a regime shift may change both the transition operator and the observation operator. For example, the start of flow changes the mapping from radial thermal coefficients to measured temperature because $T_{in}(t)$ becomes active in the wellbore energy balance.

A further refinement is useful for inversion. The radial modes can be partitioned into fast and slow thermal components. Let

$$a(t) = \begin{bmatrix} a_f(t) \\ a_s(t) \end{bmatrix}, \tag{21}$$

where a_f spans short radial scales near the wellbore and a_s spans broader, slower modes. Early-time inflow temperature is much more sensitive to a_f, while late recovery and deeper radial structure are carried by a_s. During online learning, forgetting of a_f-related dynamics is especially harmful for early

Table 9. Regularization and stability terms in the learning objective

Regularizer	Symbol	Purpose
Observation loss	ℓ_{obs}	Penalizes mismatch with temperature and pressure data
Dynamic consistency loss	ℓ_{dyn}	Enforces agreement with predicted state transitions
Memory protection term	$\mathcal{R}_{mem}$	Prevents forgetting of historical regimes
Stability regularization	$\mathcal{R}_{stab}$	Controls operator spectrum and dissipativity
Regime penalty	$\mathcal{R}_{regime}$	Limits unrealistic regime switching

Table 10. Evaluation metrics for thermal-flow inference performance

Metric	Symbol	Interpretation
Entering temperature error	E_T	Difference between predicted and reference inflow temperature
Early-time rate error	E_q	Accuracy of inferred flow during initial DST period
Regime adaptation delay	τ_{adapt}	Time required to adjust after operational change
Thermal recovery stability	S_{th}	Consistency of long-horizon thermal relaxation
Memory retention score	R_{mem}	Ability to preserve knowledge across regimes

DST interpretation, whereas forgetting of a_s affects longer-term equilibration. This separation informs the memory design developed later.

It is also valuable to represent the circulation-to-shut-in handoff explicitly. Let $a(t_s^-)$ be the coefficient vector at the end of circulation and $a(t_s^+)$ the coefficient vector at the start of shut-in [33]. Because the field is continuous, one has

$$a(t_s^+) = \Pi_c \zeta_c + \varepsilon_c, \tag{22}$$

where ζ_c is a summary of circulation history, Π_c is a linear or weakly nonlinear map obtained from thermal simulation or analytical line-source kernels, and ε_c absorbs mismatch. This relation allows the online estimator to carry information from circulation into shut-in without reinitializing the state arbitrarily. Likewise, at the onset of flow, the initial inflow temperature depends on the shut-in terminal state:

$$T_{in}(t_f^+) = T_\infty + c(t_f^+)^\top a(t_f^-). \tag{23}$$

These interface relations are precisely where fixed-regime methods often lose information. By embedding them directly in the reduced state representation, the present formulation preserves continuity across operational stages.

The reduction is therefore not merely a dimensional convenience. It is a way of encoding the physical memory of the well. The coefficients $a(t)$ summarize how far and how strongly the near-wellbore zone has been cooled or heated. The coefficients $b(t)$ summarize the remaining thermal imbalance in the wellbore. The observation operators encode how those latent imbalances appear in measured temperature, pressure, and rate under each regime [19]. Once this reduced structure is in place, online operator learning becomes possible. The next section develops that operator formulation explicitly.

4. Regime-Aware Latent Operator Formulation

The reduced thermal-flow system remains nonstationary because the well traverses several operational regimes before thermal equilibrium is restored. A central design goal is therefore to represent nonstationarity in a way that preserves shared physical structure while allowing selective correction under changing operations. The operator formulation adopted here decomposes the state transition into a common backbone and regime-specific perturbations. This yields a system that can adapt when moving from circulation to shut-in or from shut-in to flow without discarding everything learned previously.

Discretizing time at observation or update times $t_1, t_2, \ldots, t_N$, let x_k denote the latent state at time index k. The discrete reduced system is written as

$$\begin{aligned} x_{k+1} &= \bar{A}_k x_k + \bar{B}_k u_k + R_k(s_k)x_k + C_k(s_k)u_k + g_k(x_k, u_k, s_k) + \epsilon_k \\ y_k &= \bar{H}_k x_k + D_k u_k + M_k(s_k)x_k + h_k(x_k, u_k, s_k) + \eta_k. \end{aligned} \tag{24}$$

The matrices $\bar{A}_k$, $\bar{B}_k$, and $\bar{H}_k$ constitute the shared backbone, which captures the diffusion-dominated thermal structure and the baseline wellbore response. The regime corrections R_k, C_k, and M_k account for operation-specific effects. For circulation, these corrections emphasize wellbore

forcing and heat-transfer uncertainty. For shut-in, they reduce toward a nearly diffusive relaxation structure [3]. For early flow, they emphasize inflow weighting, multientry mixing, and thermal-hydraulic coupling. The nonlinear terms g_k and h_k capture moderate departures from linearity such as temperature-dependent fluid properties or rate-sensitive pressure losses.

A useful parameterization of the regime correction is low rank:

$$R_k(s_k) = \sum_{\ell=1}^{L} \pi_{k,\ell} P_{k,\ell} Q_{k,\ell}^{\top}, \tag{25}$$

where $\pi_{k,\ell}$ are regime responsibilities and $P_{k,\ell}Q_{k,\ell}^{\top}$ are low-rank operator factors. This reflects the empirical expectation that operational shifts usually alter a limited subset of dynamical directions rather than the full state space. For example, the start of flow may strongly alter the observation of near-wall thermal modes and certain hydraulic components while leaving slower radial recovery modes almost unchanged. By concentrating adaptation into low-dimensional operator corrections, the model remains both interpretable and resistant to instability.

Soft regime responsibilities are preferable to hard switching because physical transitions are often blurred. Let the regime set include circulation, shut-in, early flow, multirate flow, and buildup, with an additional novelty slot when the current measurements are not well explained by existing operator corrections. The regime weights are computed from residual likelihood, operational context, and memory compatibility:

$$\pi_{k,\ell} = \frac{\exp(\alpha_{k,\ell})}{\sum_{j=1}^{L+1} \exp(\alpha_{k,j})}, \tag{26}$$

where $\alpha_{k,\ell}$ depends on predicted observation error, latent-state compatibility with historical memory for regime ℓ, and persistence of previous regime assignments. The effective transition operator is then

$$A_k^{\mathsf{eff}} = \bar{A}_k + \sum_{\ell=1}^{L} \pi_{k,\ell} P_{k,\ell} Q_{k,\ell}^{\top} + J_{g,k}, \tag{27}$$

with $J_{g,k}$ the Jacobian of the nonlinear residual. An analogous expression holds for the effective observation operator.

The thermal substructure of A_k^{eff} deserves special treatment because it encodes diffusion-like recovery. Let the state be partitioned as [35]

$$x_k = \begin{bmatrix} a_{f,k} \\ a_{s,k} \\ b_k \\ q_k \\ \vartheta_k \end{bmatrix}. \tag{28}$$

Then the transition matrix acquires block form

$$A_k^{\mathsf{eff}} = \begin{bmatrix} A_{ff,k} & A_{fs,k} & A_{fb,k} & A_{fq,k} & A_{f\vartheta,k} \\ A_{sf,k} & A_{ss,k} & A_{sb,k} & A_{sq,k} & A_{s\vartheta,k} \\ A_{bf,k} & A_{bs,k} & A_{bb,k} & A_{bq,k} & A_{b\vartheta,k} \\ A_{qf,k} & A_{qs,k} & A_{qb,k} & A_{qq,k} & A_{q\vartheta,k} \\ 0 & 0 & 0 & 0 & I \end{bmatrix}. \tag{29}$$

The blocks $A_{ff,k}$ and $A_{ss,k}$ govern fast and slow radial thermal recovery, $A_{bf,k}$ and $A_{bs,k}$ map formation thermal state into wellbore temperature dynamics, and $A_{qf,k}$, $A_{qs,k}$ encode temperature-dependent flow or rate effects. The final identity row indicates that certain parameters may be modeled as random walks or slowly drifting states rather than fast dynamic variables. This explicit block organization makes it possible to protect especially sensitive subspaces from abrupt adaptation while allowing regime-specific corrections elsewhere.

The observation model reflects the operational meaning of temperature. Suppose the measured vector includes bottom-hole temperature T_{bh}, bottom-hole pressure p_{bh}, and total test rate q_t. Then a typical reduced observation relation is

$$y_k = \begin{bmatrix} T_{bh,k} \\ p_{bh,k} \\ q_{t,k} \end{bmatrix} = \begin{bmatrix} \bar{H}_{T,k} \\ \bar{H}_{p,k} \\ \bar{H}_{q,k} \end{bmatrix} x_k + \begin{bmatrix} M_{T,k}(s_k) \\ M_{p,k}(s_k) \\ M_{q,k}(s_k) \end{bmatrix} x_k + \nu_k. \tag{30}$$

In the early flow regime, $M_{T,k}(s_k)$ places strong weight on the inflow-temperature functional $c_k^{\top} a_k$. During shut-in, the same measured temperature may depend more directly on wellbore thermal imbalance and local relaxation. The state-space form therefore captures the fact that a sensor is not tied to a single fixed physical meaning across operations.

To regularize the model, the backbone and the regime corrections are given different temporal scales. The backbone evolves slowly:

$$\bar{A}_{k+1} = \bar{A}_k + \Delta \bar{A}_k, \qquad \|\Delta \bar{A}_k\|_F^2 \text{ small}, \tag{31}$$

while the regime corrections may evolve more rapidly but under low-rank or sparsity constraints:

$$\begin{aligned} P_{k+1,\ell} &= P_{k,\ell} + \Delta P_{k,\ell} \\ Q_{k+1,\ell} &= Q_{k,\ell} + \Delta Q_{k,\ell}, \end{aligned} \tag{32}$$

with penalties on $\|\Delta P_{k,\ell}\|_F^2$, $\|\Delta Q_{k,\ell}\|_F^2$, and possibly on their ranks. This separation reflects an intuitive physical assumption: the dominant thermal diffusion geometry of the near-wellbore zone changes slowly, whereas the way it is observed or coupled into the wellbore can change more abruptly at operational transitions [10].

A further refinement is to impose physically motivated commutation or dissipativity constraints on the thermal blocks. Let L_{th} denote the nominal reduced diffusion operator obtained from the basis projection. One may penalize deviations of the learned thermal backbone from diffusion structure:

$$\mathcal{R}_{\mathsf{diff}} = \|\bar{A}_{\mathsf{th},k} - \exp(\Delta t_k L_{\mathsf{th}})\|_F^2 + \beta_c \|\bar{A}_{\mathsf{th},k} L_{\mathsf{th}} - L_{\mathsf{th}} \bar{A}_{\mathsf{th},k}\|_F^2. \tag{33}$$

The first term keeps the backbone close to nominal thermal recovery over the time step Δt_k, and the second discourages operator distortions that would significantly alter the modal structure of diffusion. These penalties do not force exact adherence to a fixed model, but they prevent the learner from explaining recent data by inventing unphysical thermal dynamics.

The regime-aware operator representation thus provides the formal bridge between physics and adaptation. It preserves a common thermal-flow scaffold, permits low-complexity oper-

ational corrections, and localizes fast learning to the parts of the model that ought to change when the regime changes. The next section builds on this scaffold to develop an explicit continual learning and memory-consolidation strategy.

5. Physics-Constrained Continual Learning and Memory Consolidation

The problem of sequential well interpretation under circulation-induced thermal disturbance is fundamentally one of learning with memory. Information extracted during circulation and shut-in should not be lost when the well begins to flow, because that information defines the current radial thermal field and therefore the entering fluid temperature. Yet some adaptation is unavoidable once the regime changes, because the observation law and certain couplings change markedly between shut-in and early flow. The learning architecture developed in this section is designed to preserve thermally meaningful historical structure while allowing regime-specific adaptation [31].

Let Θ_k denote the collection of all learnable quantities at time k: the backbone operators, the low-rank regime corrections, selected noise covariances, and any trainable maps entering the nonlinear residuals. Let $\mathcal{M}_{k-1}$ denote the memory bank accumulated up to time $k-1$. The online objective is

$$\mathcal{J}_k(\Theta_k) = \ell_{\text{obs},k} + \lambda_x \ell_{\text{dyn},k} + \lambda_m \mathcal{R}_{\text{mem},k} + \lambda_p \|\Theta_k - \Theta_{k-1}\|^2_{W_k} + \lambda_s \mathcal{R}_{\text{stab},k} + \lambda_r \mathcal{R}_{\text{regime},k}. \tag{34}$$

The observation loss $\ell_{\text{obs},k}$ measures mismatch between measured and predicted pressure, temperature, and rate. The dynamic loss $\ell_{\text{dyn},k}$ penalizes inconsistency between updated and predicted latent states. The memory regularizer $\mathcal{R}_{\text{mem},k}$ protects regime-relevant historical structure. The parameter-motion penalty uses an importance matrix W_k to discourage harmful changes. The stability regularizer controls the operator spectrum and thermal dissipativity. The regime term penalizes implausible switching among regime assignments.

The memory bank is organized by regime but also by thermal content. For each memory slot m, define

$$\mathcal{M}_m = \left(\bar{x}_m, \Sigma_m, \bar{A}_m, \bar{H}_m, \mathcal{T}_m, \Omega_m\right), \tag{35}$$

where $\bar{x}_m$ is a representative latent-state centroid, Σ_m a covariance summary, $\bar{A}_m$ a representative effective operator, $\bar{H}_m$ a representative observation map, $\mathcal{T}_m$ a collection of reduced trajectory fragments, and Ω_m an importance matrix approximating the sensitivity of that memory′ s predictive competence to parameter motion. Importantly, the trajectory fragments in $\mathcal{T}_m$ are stored in latent thermal-flow coordinates, not as raw sensor traces alone. This makes memory storage efficient and directly aligned with the physical dynamics one wishes to preserve.

A memory slot is not created for every short-lived perturbation. Instead, a candidate regime segment becomes a new memory if it is both persistent and sufficiently different from existing memories. Let $d_{\min,k}$ be the minimal distance between the recent latent trajectory context and the existing memory centroids, and let ρ_k be a persistence statistic computed from regime responsibilities and residual consistency over a recent window. A new memory is instantiated when

$$\rho_k > \rho_{\text{th}} \quad \text{and} \quad d_{\min,k} > d_{\text{th}}. \tag{36}$$

Otherwise the closest compatible memory is updated by weighted averaging [32]. This rule prevents the bank from fragmenting into many nearly redundant slots while still allowing distinct operational situations, such as unusually prolonged cooling or atypical multirate behavior, to be retained when genuinely necessary.

The memory regularizer is composed of two parts: operator anchoring and latent replay. Operator anchoring preserves the previously learned thermal-flow structure for each important memory:

$$\mathcal{R}_{\text{anch},k} = \sum_m \gamma_{k,m} \left(\|A_k^{(m)} - \bar{A}_m\|_F^2 + \|H_k^{(m)} - \bar{H}_m\|_F^2 \right), \tag{37}$$

where $A_k^{(m)}$ and $H_k^{(m)}$ are the current effective operators obtained when memory m is activated, and $\gamma_{k,m}$ weights memory importance according to recurrence probability and forgetting risk. Latent replay evaluates the current parameters on representative stored trajectories:

$$\mathcal{R}_{\text{replay},k} = \sum_m \gamma_{k,m} \sum_{\tau \in \mathcal{T}_m} \sum_{j \in \tau} \left[\|x_{j+1}^\tau - \hat{x}_{j+1|j}^\tau(\Theta_k)\|_2^2 + \lambda_y \|y_j^\tau - \hat{y}_j^\tau(\Theta_k)$$

(38)

The total memory term is then

$$\mathcal{R}_{\text{mem},k} = \mathcal{R}_{\text{anch},k} + \beta_{\text{rep}} \mathcal{R}_{\text{replay},k}. \tag{39}$$

This construction is especially valuable for the thermal problem because operator drift can degrade the quality of early inflow temperature estimation even before observable temperature misfit on current data becomes large.

The importance matrix W_k determines which parameter directions are dangerous to modify. It is assembled from the memory-specific sensitivity matrices:

$$W_k = \sum_m \gamma_{k,m} \Omega_m + \epsilon I. \tag{40}$$

Each Ω_m can be approximated from the curvature of the replay loss or from Fisher-like information on the memory trajectories. Physically, large entries in Ω_m tend to correspond to parameters governing near-wall thermal recovery, wellbore heat transfer, and the mapping from latent radial modes to entering temperature. By penalizing motion in those directions, the learner avoids catastrophic forgetting of precisely the structure needed for later test interpretation [22].

Adaptation is split into fast and slow timescales. Fast updates affect the low-rank regime corrections and a limited set of plastic parameters:

$$\vartheta_k^{\text{fast}} = \vartheta_{k-1}^{\text{fast}} - \alpha_k \nabla_{\vartheta^{\text{fast}}} \mathcal{J}_k. \tag{41}$$

Slow updates affect the backbone and the coordinate-defining

maps:

$$\vartheta_k^{\text{slow}} = \vartheta_{k-1}^{\text{slow}} - \beta_k \nabla_{\vartheta^{\text{slow}}} \mathcal{J}_k, \qquad \beta_k \ll \alpha_k. \tag{42}$$

This separation matches the physics. The diffusion-dominated thermal backbone should not be rewritten every time a rate changes. The way that backbone is observed or coupled into the wellbore, however, may need more agile correction. By constraining fast learning to low-rank operational directions, the model remains adaptable without losing the shared thermal atlas built from earlier operations.

A further component of the continual learner is novelty handling. Sometimes the current residual pattern cannot be explained well by any existing memory. In that case the novelty slot becomes active, and a temporary operator correction is allocated. This correction is allowed to adapt quickly but is not consolidated immediately [16]. Only if the novel behavior persists and its explanatory value remains high is it promoted to a permanent memory. This prevents the memory bank from overreacting to noise, sensor glitches, or minor disturbances.

The entire learning rule is therefore guided by a simple physical principle: update aggressively only when the data supply sustained evidence that the operational mapping has changed, but preserve the latent thermal structure that determines the current state of the near-wellbore zone. The next section explains how this principle is implemented in sequential state and parameter estimation, especially when multiple entry points and transient rate changes are present.

6. Sequential Estimation, Multientry Inflow Reconstruction, and Early-Time Rate Inference

The continual learner requires a sequential inference engine capable of updating latent thermal state, hydraulic summaries, and regime responsibilities from streaming measurements. The measurements typically include a subset of bottom-hole temperatures, bottom-hole pressures, surface flow rates, and operational controls. Because the radial thermal field is never observed directly, the inference procedure must combine prediction from the reduced physical model with correction from indirect observations. It must also distribute information appropriately across multiple possible entry points in the well.

Let the filtering distribution at time k be approximated by

$$q_k(x_k, s_k) = q_k(x_k \mid s_k)\, q_k(s_k). \tag{43}$$

The regime marginal $q_k(s_k)$ is represented by the soft weights $\pi_{k,\ell}$. Conditioned on a regime, the state distribution is approximated as Gaussian or Gaussian mixture around the reduced latent state. Prediction is carried out using the regime-weighted effective operator:

$$\begin{aligned}
\hat{x}_{k|k-1} &= \bar{A}_{k-1}\hat{x}_{k-1} + \bar{B}_{k-1}u_{k-1} + \sum_{\ell} \pi_{k-1,\ell} P_{k-1,\ell} Q_{k-1,\ell}^{\top} \hat{x}_{k-1} + \hat{q}_{k-1}, \\
P_{k|k-1} &= A_{k-1}^{\text{eff}} P_{k-1} A_{k-1}^{\text{eff}\top} + Q_{k-1}.
\end{aligned} \tag{44}$$

The observation prediction is [12]

$$\hat{y}_{k|k-1} = \bar{H}_k \hat{x}_{k|k-1} + D_k u_k + \sum_{\ell} \pi_{k,\ell} M_{k,\ell} \hat{x}_{k|k-1} + \hat{h}_k. \tag{45}$$

A standard Kalman-like correction can then be applied if the nonlinearities are mild or locally linearized:

$$\begin{aligned}
K_k &= P_{k|k-1} H_k^{\text{eff}\top} \left(H_k^{\text{eff}} P_{k|k-1} H_k^{\text{eff}\top} + R_k \right)^{-1} \\
\hat{x}_k &= \hat{x}_{k|k-1} + K_k \left(y_k - \hat{y}_{k|k-1} \right) \\
P_k &= \left(I - K_k H_k^{\text{eff}} \right) P_{k|k-1}.
\end{aligned} \tag{46}$$

In situations with stronger nonlinearity, ensemble or unscented updates may be substituted, but the present form is sufficient to expose the structure of the estimator.

Multientry inflow introduces an additional inverse problem: the total wellbore rate is observed or partially constrained, but the partition among entry points and the temperature of each entering stream are latent. Let N_p denote the number of entry points. For each entry point j, define a local thermal state $a_k^{(j)}$ and local inflow temperature

$$T_{in,k}^{(j)} = T_{\infty}^{(j)} + c_k^{(j)\top} a_k^{(j)}. \tag{47}$$

The inflow mass rates $\dot{m}_k^{(j)}$ satisfy

$$\sum_{j=1}^{N_p} \dot{m}_k^{(j)} = \dot{m}_{\text{tot},k}, \tag{48}$$

where $\dot{m}_{\text{tot},k}$ may be known approximately from surface measurement or inferred jointly. A soft allocation model is useful:

$$\dot{m}_k^{(j)} = \dot{m}_{\text{tot},k} \frac{\exp(\zeta_k^{(j)})}{\sum_{i=1}^{N_p} \exp(\zeta_k^{(i)})}, \tag{49}$$

where $\zeta_k^{(j)}$ is a latent log-allocation variable influenced by pressure drawdown, skin, local mobility, and temperature-sensitive property terms. The entering enthalpy contributions then combine in the wellbore energy equation, and the measured bottom-hole temperature constrains both the $\dot{m}_k^{(j)}$ and the $T_{in,k}^{(j)}$.

A particularly important application is early-time flow inference from temperature. In many wells, temperature responds to near-wellbore thermal history in a way that can inform the effective inflow rate before pressure derivatives have fully stabilized. To exploit this, the model computes the sensitivity of bottom-hole temperature to local inflow rate:

$$\frac{\partial T_{bh,k}}{\partial \dot{m}_k^{(j)}} = \frac{\partial T_{bh,k}}{\partial T_{in,k}^{(j)}} \frac{\partial T_{in,k}^{(j)}}{\partial \dot{m}_k^{(j)}} + \frac{\partial T_{bh,k}}{\partial h_{in,k}^{(j)}} \frac{\partial h_{in,k}^{(j)}}{\partial \dot{m}_k^{(j)}}. \tag{50}$$

These sensitivities enter both the observation Jacobian and the parameter-importance structure. If the near-wellbore zone is strongly cooled, $\partial T_{bh}/\partial \dot{m}^{(j)}$ can be substantial at

early times, and temperature becomes highly informative about rate. If the zone has nearly recovered, the sensitivity weakens and temperature contributes less incremental information. Thus the value of temperature data for rate inference is itself regime dependent and mediated by the latent thermal state [34].

The estimator also uses a fixed-lag smoother to improve the thermal state during ambiguous transitions. Suppose a flow period begins shortly after shut-in. The first few observations may not be sufficient to determine the exact near-wall modal coefficients. A lag smoother over the most recent L time steps updates past states in light of new data:

$$\hat{x}_{k-\ell|k} = \hat{x}_{k-\ell|k-1} + J_{k-\ell}\left(\hat{x}_{k-\ell+1|k} - \hat{x}_{k-\ell+1|k-1}\right), \quad (51)$$

for $\ell = 1, \dots, L$, with $J_{k-\ell}$ the smoothing gain. This is especially useful because the latent thermal state evolves relatively smoothly even when the regime changes. Revising the just-prior shut-in state in light of the first flow observations can materially improve the inferred entering temperature without requiring a full retrospective batch optimization.

Regime probabilities are updated jointly with the state. A convenient approximation evaluates the filtered innovation likelihood under each regime and multiplies by a persistence prior:

$$\pi_{k,\ell} \propto \pi_{k-1,\ell}^{\rho} \exp\left(-\frac{1}{2}\nu_{k,\ell}^{\top} S_{k,\ell}^{-1} \nu_{k,\ell}\right) \Gamma_{k,\ell}, \quad (52)$$

where $\nu_{k,\ell} = y_k - \hat{y}_{k|k-1}^{(\ell)}$, $S_{k,\ell}$ is the corresponding innovation covariance, and $\Gamma_{k,\ell}$ includes operational priors such as scheduled rate changes or known pump stoppage. The resulting soft assignment allows the model to recognize, for instance, that the first moments of flow may still retain strong shut-in characteristics or that a multirate change has altered the observation mapping without fully changing the latent thermal state.

Sequential estimation in this setting is therefore not just a matter of fitting observations. It is the coordinated update of a hidden radial thermal field, multientry hydraulic allocation, and regime-conditioned observation logic [15]. The next section examines whether these updates remain stable and identifiable and under what conditions the model can be expected to converge to thermally meaningful states.

7. Stability, Identifiability, and Convergence Analysis

The sequential model described above is only useful if its learned dynamics remain stable, if its reduced latent states are sufficiently identifiable from the available measurements, and if its online updates do not accumulate error in a way that invalidates early-time interpretation. These questions are particularly important in the present field because the latent thermal variables represent a diffusion-driven physical process. A model that fits recent data but violates the underlying dissipative structure can produce plausible short windows and misleading long-horizon forecasts.

Consider the error dynamics of the filtered latent state. Let $e_k = x_k - \hat{x}_k$. Linearizing the nonlinear residual around the filtered trajectory yields

$$e_{k+1} = F_k e_k + \delta_k + \nu_k, \quad (53)$$

where $F_k = A_k^{\mathrm{eff}} - K_{k+1} H_{k+1}^{\mathrm{eff}} A_k^{\mathrm{eff}}$ is the local filtered error propagator, δ_k captures mismatch induced by parameter adaptation and regime misassignment, and ν_k aggregates process and measurement noise terms. A sufficient condition for bounded error is that the induced norm of F_k remain uniformly below one on average, with δ_k and ν_k bounded in second moment. This condition is not trivial because regime changes can alter both the state transition and the filter gain sharply. The stability regularizer is therefore designed precisely to prevent the learner from creating high-gain operator modes in response to short-term residuals.

The adaptation mismatch term can be bounded in terms of the parameter-motion metric. Let T_Θ denote the transition map under parameters Θ. Then

$$\begin{aligned} \|\delta_k\|_2 &= \|T_{\Theta_k}(\hat{x}_k, u_k) - T_{\Theta_{k-1}}(\hat{x}_k, u_k)\|_2 \\ &\le L_{\Theta,k} \|\Theta_k - \Theta_{k-1}\|_2, \end{aligned} \quad (54)$$

where $L_{\Theta,k}$ is a local Lipschitz constant. Since $\|\Theta_k - \Theta_{k-1}\|_{W_k}^2$ is penalized rather than the plain Euclidean norm, large motion is allowed primarily in directions judged less sensitive or less important to memory. This reduces the chance that the learner destabilizes the thermal dynamics while adapting to a new regime [36]. In physical terms, the model is allowed to reweight observation mappings and certain multientry couplings relatively quickly, but it is discouraged from making abrupt changes to the core diffusion-like modes of the near-wellbore recovery field.

Identifiability is limited by the fact that the radial thermal field is not directly measured. The reduced basis representation helps by imposing a physically interpretable structure, but some ambiguity remains. A formal observability analysis can be based on the empirical observability matrix over horizon h:

$$\mathcal{O}_{k,h} = \begin{bmatrix} H_k^{\mathrm{eff}} \\ H_{k+1}^{\mathrm{eff}} A_k^{\mathrm{eff}} \\ H_{k+2}^{\mathrm{eff}} A_{k+1}^{\mathrm{eff}} A_k^{\mathrm{eff}} \\ \vdots \\ H_{k+h-1}^{\mathrm{eff}} A_{k+h-2}^{\mathrm{eff}} \cdots A_k^{\mathrm{eff}} \end{bmatrix}. \quad (55)$$

If $\sigma_{\min}(\mathcal{O}_{k,h})$ is too small, certain latent directions are poorly informed by the data over that window. In practice, the fast radial modes are often more observable during early flow because entering temperature is highly sensitive to them, whereas slow radial modes may be better constrained during extended shut-in or later thermal recovery. This regime dependence of observability is precisely why a memory-based learner is useful: information gleaned about poorly observed directions in one regime can be preserved and reused in later regimes where those directions matter but are not freshly observable.

A related issue is coordinate drift. The reduced thermal state should remain comparable across time so that memory slots stay meaningful. Suppose there exists an invertible transfor-

mation S_k such that

$$x'_k = S_k x_k$$
$$A'_k = S_{k+1} A_k S_k^{-1}$$
$$H'_k = H_k S_k^{-1}. \tag{56}$$

If S_k changes substantially over time, then stored memory trajectories become difficult to interpret under the current coordinates even if current observation fit remains high. The use of explicit radial thermal bases, slow backbone updates, and operator anchoring mitigates this problem [4]. In effect, the model does not permit arbitrary latent reparameterization because the basis functions and physical state blocks provide a coordinate anchor. The remaining ambiguity is therefore smaller than in a purely generic latent model.

Convergence of the memory-constrained updates can be understood through a regret-style decomposition. Let $\Theta_k^\star$ be the hypothetical regime-aware parameter vector minimizing the instantaneous expected loss at time k. The cumulative shifted regret is

$$\mathcal{R}_N = \sum_{k=1}^{N} \left(\mathbb{E}\mathcal{J}_k(\Theta_k) - \mathbb{E}\mathcal{J}_k(\Theta_k^\star) \right). \tag{57}$$

Under smoothness of the loss, bounded parameter drift of $\Theta_k^\star$, and bounded gradient noise, the regret decomposes into terms associated with estimation error, regime change, memory protection, and computational approximation. The memory term reduces regret when earlier regimes recur or when current data alone are insufficient to reidentify poorly observed thermal directions. The price is a bias term when a truly new regime differs substantially from all stored memories. This trade-off is controlled by the novelty slot and the adaptive replay weights.

Thermal dissipativity provides an additional convergence criterion for the thermal substate. Let $x_k^{\mathrm{th}} = [a_{f,k}^\top, a_{s,k}^\top, b_k^\top]^\top$ and let $P_d \succ 0$ be a weighting matrix approximating thermal energy. Define [9]

$$V_k = x_k^{\mathrm{th}\top} P_d x_k^{\mathrm{th}}. \tag{58}$$

In the absence of external heating and with bounded inflow forcing, one expects

$$V_{k+1} - V_k \le -\mu \|x_k^{\mathrm{th}}\|_2^2 + \chi \|u_k\|_2^2 + \epsilon_k, \tag{59}$$

for some $\mu > 0$, $\chi \ge 0$, and small approximation residual ϵ_k. Enforcing or approximately satisfying such a dissipation inequality prevents the learner from encoding spurious thermal oscillations that could fit noisy data while contradicting the recovery physics. This is particularly important during shut-in, when the latent thermal state should move monotonically toward equilibrium in a suitable averaged sense.

The analysis therefore suggests three conditions for reliable use. First, the basis and observation system should provide at least intermittent observability of the important thermal modes. Second, regime-conditioned updates should remain low complexity and memory constrained so that adaptation does not destroy dissipative structure. Third, the memory bank should preserve information about weakly observed but physically important modes, especially those controlling early inflow temperature. When these conditions are satisfied approximately, the sequential learner can adapt to operational shifts while maintaining a stable and interpretable estimate of the near-wellbore thermal field.

8. Numerical Realization and Field-Oriented Experiment Design

The proposed framework is intended for practical sequential interpretation rather than only theoretical analysis, so computational design matters. The reduced state dimension must remain small enough for real-time or near-real-time updating, yet rich enough to represent the radial thermal structure that governs early inflow temperature. A typical implementation might retain between four and twelve radial thermal modes per active interval, two to six axial wellbore modes, a small set of hydraulic allocation variables, and a handful of slowly varying uncertain parameters [37]. This yields a latent dimension comfortably below that of a full radial-axial discretization while still preserving the main degrees of freedom relevant to thermal DST interpretation.

The basis construction can proceed offline. A family of circulation and recovery simulations is generated over plausible ranges of diffusivity, heat-transfer coefficient, circulation duration, shut-in time, and inflow rate. From these simulations, radial temperature snapshots are collected and compressed through a proper orthogonal decomposition or a diffusion-eigenfunction fit. The resulting basis is then orthonormalized with respect to a radial energy inner product

$$\langle f, g \rangle_r = \int_{r_w}^{r_b} f(r) g(r)\, r\, dr. \tag{60}$$

This weighting ensures that the modes respect the geometry of radial conduction rather than merely Euclidean snapshot variance. A similar procedure can be applied to wellbore temperature snapshots along the completion interval. Importantly, this offline basis construction does not require access to the exact field well being interpreted. It only defines the coordinate system in which online state estimation and memory storage will occur.

Online computation alternates among four modules. The first predicts the latent state and observation using the current backbone and regime correction [1]. The second updates the state using new pressure, temperature, and rate data. The third updates regime responsibilities and determines whether novelty is present. The fourth performs limited parameter adaptation and memory maintenance. Because the regime corrections are low rank, the dominant linear algebra costs are modest. If r is the latent dimension and q the rank of each correction, applying the effective transition costs $O(r^2 + Lrq)$, which is manageable for the dimensions envisioned here. Matrix inversions in the filter step are carried out in observation space, which is usually very small because the number of measured channels per update is limited.

A particularly valuable computational feature is that replay occurs in latent space. Suppose each memory stores ten short trajectory fragments of length twenty in a state dimension of fifteen. Then the replay burden remains negligible compared with storing or reprocessing full raw thermal histories. More

importantly, the replay is physically targeted: it preserves thermal transitions and inflow mappings rather than every sample indiscriminately. If computational budget becomes tight, replay can be prioritized for memory slots with highest forgetting risk and recurrence probability, as encoded in the weighting scheme from earlier sections [27].

The synthetic experiment design should reflect realistic operational heterogeneity. One family of cases may vary circulation duration and mud temperature so that some wells experience mild near-wellbore cooling while others experience strong cooling. Another family may vary shut-in duration so that early flow begins from significantly different recovery states. A third family may introduce multirate test schedules with one or more buildup periods. A fourth may vary the number of active entry points and the heterogeneity of local mobility. Across these families, the central questions are whether the learner preserves knowledge of the disturbed thermal field across regime shifts and whether it improves early-time entering temperature and rate inference relative to fixed-regime baselines.

Field-oriented evaluation should mimic how data arrive in practice. Temperature and pressure may be sampled at high frequency, while reliable rate estimates may be delayed or noisier. Some periods may contain missing measurements. Operational schedules such as choke changes or circulation stop times may be known, but the physical response may be delayed. The experiment design should therefore include asynchronous updates, measurement gaps, and moderate model mismatch. These features matter because a method that works only in perfectly synchronized synthetic data may fail to preserve the thermal state under realistic field conditions [8].

A valuable benchmark comparison includes at least three alternatives. The first is a fixed-parameter thermal-flow model calibrated once and then run sequentially without memory. The second is a purely adaptive online model that updates aggressively without replay or parameter-importance weighting. The third is a deterministic analytical correction model that uses a shut-in recovery law to estimate entering temperature but does not learn operator corrections across regimes. Relative to these baselines, the proposed framework should be judged on entering-temperature error, early-time rate error, regime-transition adaptation lag, long-horizon stability of thermal recovery, and recurrence forgetting during repeated operating patterns.

The numerical experiments should also test robustness to misspecified diffusivity and heat-transfer coefficients. In many field settings these quantities are uncertain and correlated. A method that merely memorizes nominal coefficients will not be reliable. The proposed learner should instead use memory to preserve the thermal history while allowing parameter corrections when the data consistently support them. Sensitivity analyses can reveal whether the low-rank regime corrections absorb such uncertainty appropriately or whether the backbone becomes overloaded by parameter mismatch.

Finally, the implementation should report not only forecast accuracy but also operator diagnostics [20]. For example, one may track the dominant singular values of the thermal subblock, the magnitude of regime corrections, the number of active memory slots, and the replay burden over time. These diagnostics help determine whether improved performance arises from physically plausible operator adaptation or from hidden complexity growth. In an operational setting, such transparency is valuable because interpreters are more likely to trust a method whose internal changes remain consistent with thermal intuition.

9. Discussion

The framework proposed in this paper departs from standard well-test thermal interpretation in one essential respect: it treats operational history as something that must be learned and preserved inside the dynamical model rather than applied as an external correction. This distinction matters because near-wellbore thermal recovery is not a nuisance superposed on an otherwise stationary test. It is the medium through which early-time inflow is filtered. If that medium is poorly represented, even high-quality pressure and temperature measurements can lead to biased conclusions about fluid entry conditions and effective rate.

A useful way to view the method is as a structured compromise between deterministic thermal simulation and unrestricted data-driven adaptation. The deterministic side contributes the radial diffusion physics, the wellbore energy balance, and the definition of a physically meaningful reduced basis. The adaptive side contributes regime-conditioned operator corrections, online parameter updates, and memory-based protection against forgetting. Neither side alone is fully satisfactory [25]. Pure deterministic models often require repeated recalibration when the operation changes and may struggle when measurement meaning changes across regimes. Purely flexible adaptive models can fit recent data but risk destroying the latent thermal history that gives the data physical meaning. The present framework tries to retain the advantages of both while limiting their respective weaknesses.

The memory principle introduced here is also field specific in a useful sense. What is stored is not merely a sequence of measurements or generic embeddings. It is a compressed record of thermal trajectories, reduced operators, and sensitivity structure tied to the well' s own disturbed near-wellbore behavior. This choice reflects the fact that in subsurface thermal interpretation, the most important historical information is usually not an isolated sample but an evolving state. A short record of the radial cooling profile and its associated entering-temperature map may be more valuable than a much longer record of raw wellhead data if the goal is to interpret a later return to flow.

There are, however, clear limitations. The reduced basis approach depends on the assumption that a modest number of thermal modes can represent the operationally relevant disturbance. This is likely to hold near the tested interval in many cases, but strongly heterogeneous formations, complex completions, or multiphase compositional effects may require richer state representations. The low-rank regime corrections likewise assume that regime changes alter only a subset of dynamical directions [24]. If the physical transition is more global than that, additional flexibility may be needed. Another limitation is that the method, like all reduced inverse models, depends on having some channels of temperature and pressure data that remain informative across the operational sequence. Severe measurement sparsity will reduce observability no matter how sophisticated the memory design.

The approach is also conservative by construction. Spectral

shaping, operator anchoring, and importance-weighted parameter penalties are intended to prevent catastrophic forgetting and instability. The cost is that adaptation to a truly novel regime may initially be slower than in an unrestricted online fit. In an operational context this is often acceptable because false adaptation can be expensive: once the model has overwritten a plausible thermal history, later early-time interpretation may be difficult to recover. Still, practical deployment would benefit from adaptive tuning of novelty thresholds and replay strength based on confidence and operational priorities.

A final point concerns interpretability. Because the model uses explicit thermal modes and operator blocks with identifiable physical roles, its internal states can be related to near-wall cooling, broader radial recovery, wellbore thermal imbalance, and entry-temperature sensitivity. This is an advantage over black-box sequence models [11]. Yet those states remain reduced abstractions. They should be interpreted as thermally meaningful summaries rather than direct measurements of the rock. Used in that spirit, the framework can support more informed DST interpretation by showing not only what the current predicted entering temperature is, but also which part of the thermal history is driving it and how much of that history has been preserved from earlier regimes.

10. Conclusion

This paper presented a new research formulation for interpreting circulation-disturbed wells under changing operational regimes. The method combined reduced radial thermal dynamics, wellbore energy transport, multientry inflow representation, and physics-constrained continual learning in a single operator framework. By treating the near-wellbore temperature disturbance as a latent state with memory, the model preserved information learned during circulation and shut-in and reused it during early flow and multirate drill stem testing. The resulting architecture was specifically designed to reduce the loss of thermal history that can bias entering temperature and rate interpretation when conventional fixed-regime estimators are applied too soon after circulation.

The analysis developed the governing thermal and flow equations, constructed a reduced state representation, introduced a regime-aware latent operator decomposition, formulated a memory-based online objective, derived sequential estimation rules for state and multientry inflow allocation, and examined stability, identifiability, and computational realization. Across these components, the recurring principle was that adaptation should occur mainly in low-complexity operational directions, while the backbone of the thermal recovery process should remain physically constrained and historically informed.

In wells where near-wellbore cooling persists into test operations, the interpretation problem is inherently sequential and history dependent. A framework that preserves and updates thermal memory explicitly is therefore a natural complement to established thermal modeling practice. The method developed here offers one such framework and provides a basis for future work on richer multiphase energy models, more detailed completion architectures, and field deployment with streaming downhole measurements [28].

References

[1] Herlan Adim. Dst data evaluation in practice. *Scientific Contributions Oil and Gas*, 25(3):2–13, 3 2022.

[2] M. Al-Dawaish, N. Khochbar, F. Al-Azmi, A. Al-Otaibi, H. Ayyad, H. Mehta, J. Zacharia, A. Zaher, A. Gisolf, F. Dubost, M. Metwally, M. Yahmadi, and A. Al-Dosarry. New generation sampling and deep transient testing (dtt) proves significant presence of oil in the partitioned zone. In *Middle East Oil, Gas and Geosciences Show (MEOS GEO)*. SPE, 9 2025.

[3] Andrew G. Alpha. Genou trend–structural feature on sweetgrass arch, montana: Abstract. *AAPG Bulletin*, 39(4):532–532, 1955.

[4] F. Arachman, F. Utami, A. Wasonoaji, and D. Tobing. Brownfield redevelopment strategies in offshore north west java. In *SPE/IATMI Asia Pacific Oil & Gas Conference and Exhibition*. SPE, 10 2017.

[5] Sadegh Asadi, Khalil Rahman, Hoanh Van Pham, Thao Le Minh, and Andy Butt. Sand production assessment considering the reservoir geomechanics and water breakthrough. *The APPEA Journal*, 55(1):215–224, 6 2015.

[6] H.O. Balan and F. Gumrah. Enhanced coalbed methane recovery with respect to physical properties of coal and operational parameters. In *Canadian International Petroleum Conference*. PETSOC, 6 2008.

[7] B. Bennett and Steve Larter. Polar non-hydrocarbon contaminants in reservoir core extracts. *Geochemical Transactions*, 1(1):34–37, 8 2000.

[8] P. Birkle, P.D. Jenden, and J.M. Al-Dubaisi. Origin of formation water from the unayzah and khuff petroleum reservoirs, saudi arabia. *Procedia Earth and Planetary Science*, 7:77–80, 2013.

[9] Stefano Cantini, Davide Baldini, Enzo Beretta, Daniele Loi, and Stefano Mazzoni. Reservoir permeability from wireline formation testers. *EAGE Annual Conference & Exhibition incorporating SPE Europec*, 6 2013.

[10] William L. Dam. Geochemistry of ground water in the gallup, dakota, and morrison aquifers, san juan basin, new mexico. 1995.

[11] Thiago de Almeida Pontes. Case study: Downhole testing tools for formation evaluation in high- pressure and high-temperature environments. *IADC/SPE Drilling Conference and Exhibition*, 2 2010.

[12] Jane Negus de Wys. Geopressured habitat: A literature review, 9 1992.

[13] B. Filippi and R.J. Watson. The advantages of production testing at variable rates. In *SPE Asia-Pacific Conference*. SPE, 11 1991.

[14] Hakim Gabtni, Badia Chulli Zenatti, Chokri Jallouli, Kevin L. Mickus, and Mourad Bédir. The crustal structure of the sahel basin (eastern tunisia) determined from gravity and geothermal gradients: implications for petroleum exploration. *Arabian Journal of Geosciences*, 4(3):507–516, 4 2010.

[15] Eugene Greenwood. Oil and gas possibilities in pedregosa basin: Abstract. *AAPG Bulletin*, 55(3):536–537, 1971.

[16] Bernold M. Hanson. Bar-mar field, the tricky devonian: Abstract. *AAPG Bulletin*, 51(1):166–167, 1967.

[17] Abu Rashid Hasan, Kaushik Manikonda, Minsoo Jang, Mohammad Azizur Rahman, and Gibran Hashmi. Estimating near-wellbore cooling due to drilling circulation and its effect on drill stem test. In *SPE Annual Technical Conference and Exhibition?*, page D021S015R003. SPE, 2024.

[18] G.M. Hashmi, C.S. Kabir, and A.R. Hasan. Design and interpretation of transient tests at well's inception. *Journal of Petroleum Science and Engineering*, 145:573–584, 2016.

[19] Jerrold Horne. Engineering evaluation for development of a heavy oil reservoir in an offshore environment. In *Proceedings of Offshore South East Asia Show*. Society of Petroleum Engineers, 1986.

[20] Quan Hua Huang, Xing Yu Lin, Zhi xing Yang, Ke feng Lu, and Xian kang Hu. Productivity testing and analysis of low permeability and thick layer of n gas field. *E3S Web of Conferences*, 213:02002–, 12 2020.

[21] R. C. Leonard. Distribution of sub-surface pressure in the norwegian central graben and applications for exploration. *Geological Society, London, Petroleum Geology Conference Series*, 4(1):1295–1303, 1993.

[22] Sumei Li, Xiongqi Pang, Zhijun Jin, Haijun Yang, Zhongyao Xiao, Qiaoyuan Gu, and Baoshou Zhang. Petroleum source in the tazhong uplift, tarim basin: New insights from geochemical and fluid inclusion data. *Organic Geochemistry*, 41(6):531–553, 2010.

[23] A. W. Lindner. Oil and gas developments in australia in 1985. *AAPG Bulletin*, 70(10):1611–1624, 1986.

[24] D. Ling, S. Daungkaew, M. Kristensen, M. Lefranc, A. Sherik, C. Cavalleri, N. Hademi, A. Gisolf, M. Etchebes, F. Dubost, T. Nordin, M. A. Abu Talib, L. W. Ong, E. Motaei, and S. K. T. Rajan. Driving deep transient testing with a complete digital workflow –a sustainable exploration in green fields. In *International Petroleum Technology Conference*. IPTC, 2 2024.

[25] J. W. Lloyd, K. R. Rushton, and P. A. Jones. An assessment of groundwater inflow into a proposed shaft and drift in the warwickshire coalfield using packer test data in an electrical analogue model. *International Journal of Mine Water*, 2(4):1–18, 1983.

[26] M.J. Mavor, J.C. Close, and R.A. McBane. Formation evaluation of exploration coalbed methane wells. In *Annual Technical Meeting*. PETSOC, 6 1990.

[27] Jerry W. Mercer, Richard L. Beauheim, Richard P. Snyder, and George M. Fairer. Basic data report for drilling and hydrologic testing of drillhole doe-2 at the waste isolation pilot plant (wiip) site, 4 1987.

[28] Kentner S. Novakowski and Gregory S. Bickerton. Borehole measurement of the hydraulic properties of low-permeability rock. *Water Resources Research*, 33(11):2509–2517, 1997.

[29] Michael O'Keefe, Kaare Otto Eriksen, Stephen Williams, Dag Stensland, and Ricardo Vasques. Zero percent contamination of reservoir fluid samples achieved by focused sampling. In *SPE Asia Pacific Oil & Gas Conference and Exhibition*. SPE, 9 2006.

[30] KENNETH E. PETERS and PHILIP H. NELSON. *Criteria to Determine Borehole Formation Temperatures for Calibration of Basin and Petroleum System Models*, pages 5–15. SEPM (Society for Sedimentary Geology), 2012.

[31] N M Rahman, Sukru Sarac, and Bertrand Theuveny. Understanding pitfalls of non-reservoir effects on pressure transient-test data to avoid misleading interpretation. In *SPE Annual Technical Conference and Exhibition*. SPE, 10 2020.

[32] Ralph W. Teller and Daniel T. Chafin. Selected drill-stem test data for the upper colorado river basin. 1986.

[33] H. Vo Thanh, Yuichi Sugai, Ronald Nguele, and Kyuro Sasaki. A new petrophysical modeling workflow for fractured granite basement reservoir in cuu long basin, offshore vietnam. In *81st EAGE Conference and Exhibition 2019*, volume 2019, pages 1–5. European Association of Geoscientists & Engineers, 2019.

[34] D. van As, W. Bottomley, and J. P. Furniss. The characterisation of differential depletion in a thinly layered coal seam gas reservoir using packer inflation bleed off tests pibots. In *SPE/IATMI Asia Pacific Oil & Gas Conference and Exhibition*. SPE, 10 2017.

[35] Mingwen Wang, Gang Luo, Feng Qin, Zonghu Liao, Shuhong Zhou, and Nianfa Yang. Numerical simulation of pore pressure change caused by hydrocarbon generation in chezhen sag and its influence on hydrocarbon accumulation, 6 2023.

[36] Mingwen Wang, Gang Luo, Feng Qin, Zonghu Liao, Shuhong Zhou, and Nianfa Yang. Numerical simulation of pore pressure change caused by hydrocarbon generation in chezhen sag and its influence on hydrocarbon accumulation. *Processes*, 11(7):1976–1976, 6 2023.

[37] Amane Waseda, Hirotsugu Iwano, and Yasuyuki Asari. Migration and accumulation of hydrocarbons in the kitakanbara area, niigata, japan, based on gas carbon isotope compositions. *Journal of the Japanese Association for Petroleum Technology*, 76(1):43–51, 2011.